Reaction Kinetics, Mechanisms and Catalysis (2024) 137:1911–1925
https://doi.org/10.1007/s11144-024-02622-0

Insight into the competitiveness of C–C coupling reactions of 5-hydroxymethylfurfural with lignocellulosic compounds in one pot

Linyan Song[1] · Genkuo Nie[1,2] · Xiulei Chen[1] · Hongyu Wang[3] · Shiwei Liu[1] · Hailong Yu[1] · Xuguang Liu[4] · Guihua Yang[2] · Shitao Yu[1]

Received: 10 March 2024 / Accepted: 29 March 2024 / Published online: 29 April 2024

Abstract

The multifunctional groups of 5-hydroxymethylfurfural (5-HMF) make it could extend carbon chain by different C–C coupling reactions and extensively applied in the bio-jet fuel synthesis. Herein, one-pot reaction of lignocellulose derived chemicals with 5-HMF was studied by experimental and density functional theory (DFT) methods. The kinetic models of products were established and the apparent activation energies of the products by C–C coupling reaction of phenol, anisole, guaiacol, cyclohexanone and acetone with 5-HMF on Hβ were 95.3 kJ/mol, 104.8 kJ/mol, 90.4 kJ/mol, 90.0 kJ/mol and 112.2 kJ/mol, indicating these reactions centering on 5-HMF competitive intensively. Then the effects of the catalysis were analyzed by applying commercial catalysis to the mixed coupling reaction of 5-HMF. It was found that Brønsted acid is more favorable to alkylation reaction, and Lewis acid is more beneficial to aldol condensation reaction. By Fukui function, due to the nucleophilic index of cyclohexanone (2.74 eV) is higher than that (2.48 eV) of acetone, and the Mulliken electronegativity (3.43 eV) is weaker than that (3.55 eV) of acetone, cyclohexanone is more conducive than acetone to the aldol condensation reaction. This work provides data reference for product regulation in the bio-jet fuel synthesis.

Keywords Alkylation · Aldol condensation · Solid acid · Bio-jet fuel · Competitive one-pot reaction · Fukui function

Introduction

Nowdays, fossil resource is still the main source to meet our needs for energy, chemicals and materials [1]. However, fossil resource is non-renewable and the consume has cause energy crisis, environmental pollution and global climate change. To solve these problems, it is urgent to develop renewable sources to replace fossil ones. In

Extended author information available on the last page of the article

this context, lignocellulose is drawing much attention due to its potential for use in fuels and chemicals.

Lignocellulose is mainly composed of about 30–50% cellulose, 20–40% hemicellulose and 15–25% lignin and it is the main component of plant wall. With the development of cellulose-first biorefineries [2] and lignin-first depolymerization [3] of lignocellulose, lignocellulose can be depolymerized into sugar (e.g., glucose, fructose), acids (e.g., gluconic acid, formic acid, lactic acid, levulinic acid), ketones (e.g., acetone, cyclohexanone), aldehydes (e.g., 5-hydroxymethylfurfural, furfural), furan (e.g., furan, tetrahydrofuran), phenols (e.g., phenol, guaiacol) and aromatic oligomer (e.g., polycarbonate, polyester, polyether). Importantly, unless specially treated, what we usually get is a mixture of various chemicals [4].

Among these chemicals, 5-hydroxymethylfurfural (5-HMF) is one of the most widely studied chemicals. Various catalysts, such as deep eutectic solvents (DES) [5], solid catalyst [6, 7], homogeneous catalyst [8], etc. have been employed to directly hydrolyze cellulose/hydrolyze glucose/fructose/sucrose to obtain 5-HMF with yields ranging from 36.5 to 85.6%. 5-HMF can also be further converted to various chemicals, including levulinic acid [9], 5-acetoxymethylfurfural [10], 5-ethoxymethylfurfural [11], 2,5-diformylfuran [12], and fuels [13]. The hydroxyl group, aldehyde group and a furan ring give 5-HMF the ability to extend the carbon chain by alkylation and aldol condensation to make transport fuel precursors. Acid catalysts, such as zeolites [14], polymers [15], metal halides [16] and heteropoly acids [17] have been intensively applied in the alkylation reaction of 5-HMF with aromatic compounds. Alkaline catalysts, such as NaOH [18], MgZr [19], and acid catalysts [20] are commonly used in the aldol condensation of 5-HMF/ketones with acetone, cyclohexanone, cyclopentanone, etc. Actually, the alkaline catalyst hydrotalcite [21] and the acidic catalyst Al-DTP@ZIF-8 [22] have been used to catalyze the aldol condensation reaction of 5-HMF with acetone to form jet fuel precursors 4-[5-(hydroxymethyl)-2-furanyl]-3-buten-2-one and 1,5-bis[(5-hydroxymethyl)-2-furanyl]-1,4-penta-dien-3-one. Subsequently, the multi-functional Pd/$NbOPO_4$ [23] efficiently catalyzes the precursors to produce C9–C15 liquid alkanes by hydrogenation under mild conditions. That is, acid catalyst can catalyze both alkylation of 5-HMF with aromatic compounds and aldol condensation of 5-HMF with ketones, which give the potential to achieve a pot reaction of the feedstock blending of lignocellulosic to make jet fuel precursors. However, the competition between the reactions affects the products distribution and in turn affects the composition of the final fuel [24]. This is an interesting point, and until now there is no discussion about the competing C–C coupling reactions about 5-HMF with many compounds in one-pot by acid catalyst to grow carbon chain for making jet fuel.

Acid catalyst, especially the solid acid is the research hotspot in C–C coupling reactions, such as metal oxide, acid resin, heteropoly acid and especially zeolites. Due to zeolites have much and strong acid sites, large specific area, high ion exchange capacity, medium and high thermal stability and hydrothermal stability, it has been widely applied in acid catalyzed industrial reactions. Especially, Hβ has a three-dimensional skeleton with 12-membered ring channels, where the intersection of the channels provides sufficient space for reactions [25]. Compared with the widely used HZSM-5 zeolite, Hβ has a larger pore size, which allows di- to

tri- condensed compounds to enter into or get out the pores of the catalysis in the reaction. Compared with mesoporous zeolite MCM-41, Hβ has a higher concentration of acid sites and abundant acid type ratio [26], which can provide more reaction sites for acid-catalyzed reactions [27]. Recently, modified β zeolite has been used to catalyze the aldol condensation reaction of furfural with acetone [28] and the alkylation reaction of phenol with cyclohexanol [29] to produce 4-(2-furyl)-3-buten-2-one, 1,5-di-2-furanyl-1,4-pentadien-3-one, monoalkylphenol and dicyclohexylphenol. The selectivity can be as high as 97% and the yield can reach up to 83.4%.

In this paper, one-pot C–C coupling reactions of 5-HMF with other lignocellulose derived chemicals (phenol, anisole, guaiacol, cyclohexanone and acetone) were catalyzed by Hβ, and the competition was investigated by combining experimental and theoretical calculation. Under solvent-free conditions, reaction kinetics were studied at different temperatures with a molar ratio of 1:10 of 5-HMF to other reactants and kinetic models of coupled products were established. The reaction rate constants and activation energies for various coupled products in different reactions were calculated and compared. Then, the density functional theory (DFT) is used to further understand the competitiveness of 5-HMF with cyclohexanone and acetone catalyzed by Hβ. Moreover, the relevance of reaction with the acid properties of the catalysis was analyzed. This work provides data reference for predicting and regulating product distribution of one-pot reaction centered on 5-HMF with lignocellulosic chemicals.

Experimental

Materials

5-HMF (99.0%) was purchased from Aladdin (Shanghai, China). Cyclohexanone (≥99.5%) was purchased from Shanghai Titan Technology Co., Ltd. Phenol (≥99.0%) was purchased from Sinopharm Chemical Reagent Co., Ltd. Anisole (99.0%) was purchased from Tianjin BASF Chemical Co., Ltd. Guaiacol (98.0%) was purchased from Sarn Chemical Technology (Shanghai) Co., Ltd. Acetone (≥99.5%) was purchased from Liaodong Fine Chemical Co., Ltd. Isooctyl alcohol (>99.0%) was purchased from Shanghai Maclin Biochemical Technology Co., Ltd. Phosphotungstic acid (HPW) was purchased from Shanghai Yuanfan Biotechnology Co., LTD. Si-MCM-41, Hβ ($SiO_2/Al_2O_3=25$) and γ-Al_2O_3 were purchased from Tianjin Nankai University Molecular Sieve Factory. 80%HPW/MCM-41 catalyst was synthesized according to our previous work [30].

Catalyst characterization

The Bruno–Emmett–Teller (BET) specific surface area and pore structure of the catalyst were analyzed by N_2 physical adsorption method at -196 °C (Micomeritics ASAP 2020). Ammonia temperature-programmed adsorption–desorption (NH_3-TPD) experiments were carried out with argon as the carrier gas, and the

structural properties and acid amount of the catalyst were obtained. The type of acid was determined by pyridine adsorption infrared spectroscopy (Py-IR).

Catalytic reactions and product analysis

5-HMF (0.76 g) and phenol (5.65 g)/anisole (6.49 g)/guaiacol (7.45 g)/cyclohexanone (5.89 g)/acetone (3.48 g) reacted separately, or 5-HMF (0.76 g) and phenol (0.98 g), anisole (1.22 g), guaiacol (1.39 g), cyclohexanone (1.10 g), acetone (0.65 g) were mixed as well as Hβ (0.20 g) were placed in a 30 mL three-neck flask to react at 343.15 (±1 k), 353.15 (±1 k) and 363.15 (±1 k) for different time. The reaction products were qualitatively and quantitatively analyzed. Agilent 7890B/5975C gas chromatograph-mass spectrometer (GC–MS) equipped with HP-5 capillary column (30 m × 0.32 mm × 0.25 μm) was used for qualitative analysis, and gas chromatograph (GC-2010 Pro) equipped with FID detector and HP-5 capillary column (30 m × 0.32 mm × 0.25 μm) was used for quantitative analysis. Isooctyl alcohol was used as the standard substance and the internal standard curve of 5-HMF (Fig. S1) was established.

Computational methods

All calculations are performed using a Gaussian 16 revision C.01 [31]. The nucleophilicity index and mulliken electronegativity of cyclohexanone and acetone was predicted by B3LYP/6-31G* basis set combined with Fukui function to illustrate the competitiveness of 5-HMF in the aldol condensation reaction with cyclohexanone and acetone. Analysis of the nucleophilicity index and mulliken electronegativity is carried out with the help of Multiwfn 3.8 (dev) software [32].

Results and discussion

One-pot reaction of 5-HMF

Herein, the C–C coupling reaction of 5-HMF with phenol, anisole, guaiacol, cyclohexanone and acetone were mixed was monitored to observe the reaction evolution process. Five main reactions were detected and shown in Fig. 1a and the products are named as P1, P2, P3, P4 and P5 (Fig. S2). Analysis of all products is performed using AMDIS software. All the products are mainly crossed monocondensation products about 5-HMF with other lignocellulosic compounds due to the excessive of phenol, anisole, guaiacol, cyclohexanone and acetone. As shown in Fig. 1a, the hydroxyl groups of 5-HMF undergoes alkylation with phenol, anisole and guaiacol to form the corresponding alkylation product P1, P2 and P3. The aldehyde group of 5-HMF underwent aldol condensation reaction with cyclohexanone and acetone to generate the corresponding condensation products P4 and P5.

The conversion of 5-HMF and the selectivity of the products are shown in Table S1, and the product evolution process is described in Fig. 1b. Along with the time, the

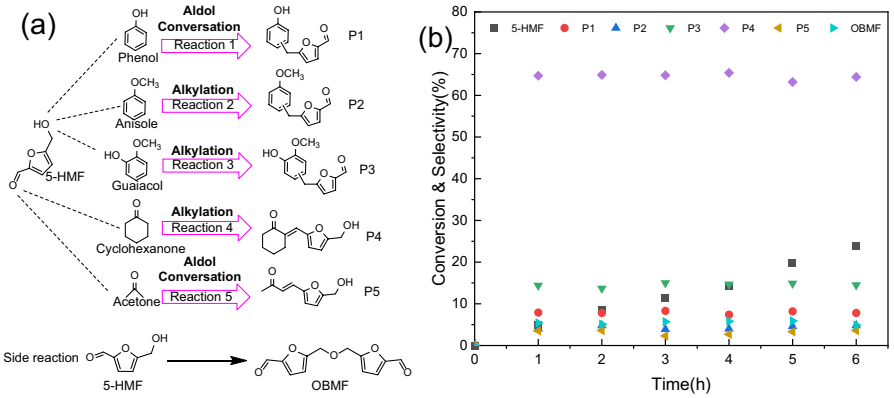

Fig. 1 The C–C coupling reaction of 5-HMF with other lignocellulose-derived chemicals (**a**) and the reaction trend of the mixed reaction of 5-HMF with phenol, anisole, guaiacol, cyclohexanone and acetone on Hβ (**b**). Reaction conditions in **b** 5-HMF (0.76 g), phenol (5.65 g), anisole (6.49 g), guaiacol (7.45 g), cyclohexanone (5.89 g), acetone (3.48 g), Hβ (0.20 g), 363.15 k

conversion of 5-HMF increases gradually in line and the selectivity of all compounds are relatively stable after 1 h with the selectivity of P4 > P3 > P2 > P1 > P5. It is worth noting that the selectivity of P4 is much higher than that of the others. Here, reaction 1, 2 and 3 are alkylation reactions of 5-HMF with the similar structure of feedstock. The activity of aromatic compounds in the alkylation reactions follow the order of guaiacol > phenol > anisole. This is attributed to the fact that the aromatic ring in guaiacol is more electron-rich than others due to the presence of –OH and $–OCH_3$, two electron-donating groups, which make aromatic ring more nucleophilic in the alkylation. Additionally, the conversion of anisole is lower than phenol because of the lower electron-donating ability of $–OCH_3$ than –OH [16]. Although reaction 4 and reaction 5 are aldol condensation, the product selectivity varies greatly and the product selectivity of P5 having much lower selectivity than P4.

In order to figure out the competition of these reactions, firstly, the reaction activation energies were obtained by experiment. Here, the reactions of 5-HMF with cyclohexanone, guaiacol, phenol, anisole and guaiacol at molar ratio of 1:10 were conducted under relative low temperatures. Based on the excessive amounts of cyclohexanone, guaiacol, phenol, anisole and guaiacol compared to 5-HMF, all the reactions are first-order reactions for the conversion of 5-HMF [33]. Thus, according to Eqs. 1–5, the rate of product formation is proportional to the concentration of 5-HMF in this experiment.

$$\frac{dC_{P1}}{dt} = k_1 C_A \tag{1}$$

$$\frac{dC_{P2}}{dt} = k_2 C_A \tag{2}$$

$$\frac{dC_{P3}}{dt} = k_3 C_A \tag{3}$$

$$\frac{dC_{P4}}{dt} = k_4 C_A \tag{4}$$

$$\frac{dC_{P5}}{dt} = k_5 C_A \tag{5}$$

At the beginning,$C_{P1,0} = C_{P2,0} = C_{P3,0} = C_{P4,0} = C_{P5,0} = 0$. According to stoichiometric relationship, $C_{P1} + C_A = C_{A,0}$, $C_{P2} + C_A = C_{A,0}$, $C_{P3} + C_A = C_{A,0}$, $C_{P4} + C_A = C_{A,0}$, $C_{P5} + C_A = C_{A,0}$, where $C_{A,0}$ represents the initial concentration of 5-HMF, C_A denotes the concentration of 5-HMF at time t. C_{P1}, C_{P2}, C_{P3}, C_{P4}, C_{P5} are the concentrations of condensation products of cyclohexanone, guaiacol, phenol, anisole and acetone with 5-HMF in Reaction 1-Reaction 5 (Fig. 1a). k_1, k_2, k_3, k_4, k_5 are the reaction rate constants for the formation of condensation products of phenol, anisole, guaiacol, cyclohexanone and acetone with 5-HMF, k only changes with the change of reaction temperature.

In order to determine the product selectivity and reaction kinetic rate constant, a series of experiments were conducted. Condensation reactions were performed at three different temperatures: 343.15 K, 353.15 K, 363.15 K. Because temperature has a significant impact on both the reaction rate and the product selectivity. 5–6 samples were taken and analyzed at various time for each reaction. The measured composition and concentration of the products at various time and temperature (343.15 K, 353.15 K, 363.15 K) were collected (Table S2-S6). The reaction data obtained from the experiment were fitted by the kinetic model proposed in Eqs. 1–5 with the help of MATLAB program [34]. The program solves the problem of nonlinear least square fitting by Isqnonlin function, and draws the fitting curve of reaction rate by fifth order Rung-Kutta method. The results of the fitting are presenting in Fig. S3-S7, and Table 1 showcases the high determination coefficients (R^2), indicating the excellent agreement between the kinetic models and experimental data. From the fitting results, reaction rate constants for each reaction product at various temperatures are obtained and summarized in Table 1. The correlation coefficients consistently exceed 0.90, ensuring the precision of the simulation. Notably, the reaction rate constants follow the order $k_4 > k_3 > k_1 > k_2 > k_5$ at identical temperatures, with reaction rates increasing as the temperature rises.

The k_1, k_2, k_3, k_4 and k_5 represent the reaction rate constants of 5-HMF with phenol, anisole guaiacol, cyclohexanone and acetone at different temperatures. $R_1{}^2$, $R_2{}^2$, $R_3{}^2$, $R_4{}^2$ and $R_5{}^2$ represent the coefficient of determination of the fitting curves of the concentration of the reaction product of 5-HMF with phenol, anisole guaiacol, cyclohexanone and acetone over time.

The Arrhenius equation is an empirical formula for the relationship between the reaction rate constant and temperature, as shown in Eq. 6. In this system, since the product is determined, the pre-exponential factor (A) and the molar

Table 1 The estimated rate constants (k) and the corresponding correlation coefficient R^2 of the products formed by the reaction of 5-HMF with phenol, anisole guaiacol, cyclohexanone and acetone at different temperatures

Temperature (K)	343.15	353.15	363.15
k_1	$2.31\ (\pm 0.18)\times 10^{-3}$	$6.96\ (\pm 0.32)\times 10^{-3}$	$1.31\ (\pm 0.14)\times 10^{-2}$
k_2	$1.71\ (\pm 0.05)\times 10^{-3}$	$6.52\ (\pm 0.20)\times 10^{-3}$	$1.28\ (\pm 0.04)\times 10^{-2}$
k_3	$2.33\ (\pm 0.21)\times 10^{-3}$	$7.08\ (\pm 0.16)\times 10^{-3}$	$1.33\ (\pm 0.11)\times 10^{-2}$
k_4	$1.03\ (\pm 0.07)\times 10^{-2}$	$3.20\ (\pm 0.18)\times 10^{-2}$	$5.83\ (\pm 0.30)\times 10^{-2}$
k_5	$1.40\ (\pm 0.08)\times 10^{-3}$	$4.39\ (\pm 0.06)\times 10^{-3}$	$1.12\ (\pm 0.08)\times 10^{-2}$
$R_1{}^2$	0.968	0.994	0.922
$R_2{}^2$	0.900	0.922	0.998
$R_3{}^2$	0.993	0.974	0.949
$R_4{}^2$	0.998	0.933	0.956
$R_5{}^2$	0.985	0.966	0.964

gas constant (R) are constants, so using the reaction rate constants at different temperatures, the apparent activation energy (Ea) can be obtained by using this equation.

$$-\ln k = \frac{E_a}{RT} - \ln A \tag{6}$$

The Arrhenius plots are constructed by plotting the negative natural logarithm of the reaction rate constant (-ln k) with the reciprocal of the temperature, and the apparent activation energy (Ea) is determined, the slope obtained by plotting is the apparent activation energy (Ea). The Arrhenius plots of the reaction products of the five reactions on Hβ are shown in Fig. 2. The activation energy (Ea) and the correlation coefficient (R^2) obtained from the Arrhenius curve are recorded in Table 2. The R^2 values are higher than 0.90, which confirmed the fitting of kinetic data. The respective apparent activation energies are 95.3 kJ/mol for P1, 104.8 kJ/mol for P2, 90.4 kJ/mol for P3, 90.0 kJ/mol for P4 and 112.2 kJ/mol for P5 (Table 2, indicating the reactions occurs from easy to hard in the order follows reaction 4 > reaction 3 > reaction 2 > reaction 1 > reaction 5. Reasonably, the selectivity of P4 is the highest and selectivity of P5 is the lowest in the mixture reaction.

The Ea_1, Ea_2, Ea_3, Ea_4 and Ea_5 represent the reaction rate constants of 5-HMF with phenol, anisole guaiacol, cyclohexanone and acetone at different temperatures. $R_1{}^2$, $R_2{}^2$, $R_3{}^2$, $R_4{}^2$ and $R_5{}^2$ represent the coefficient of determination of the fitting curves of the concentration of the reaction products of 5-HMF with phenol, anisole guaiacol, cyclohexanone and acetone over time.

Regulation products distribution by catalysis

Actually, the competitive relationship between these reactions is closely related to the properties of catalyst. As shown in the Fig. 3, the conversion of 5-HMF

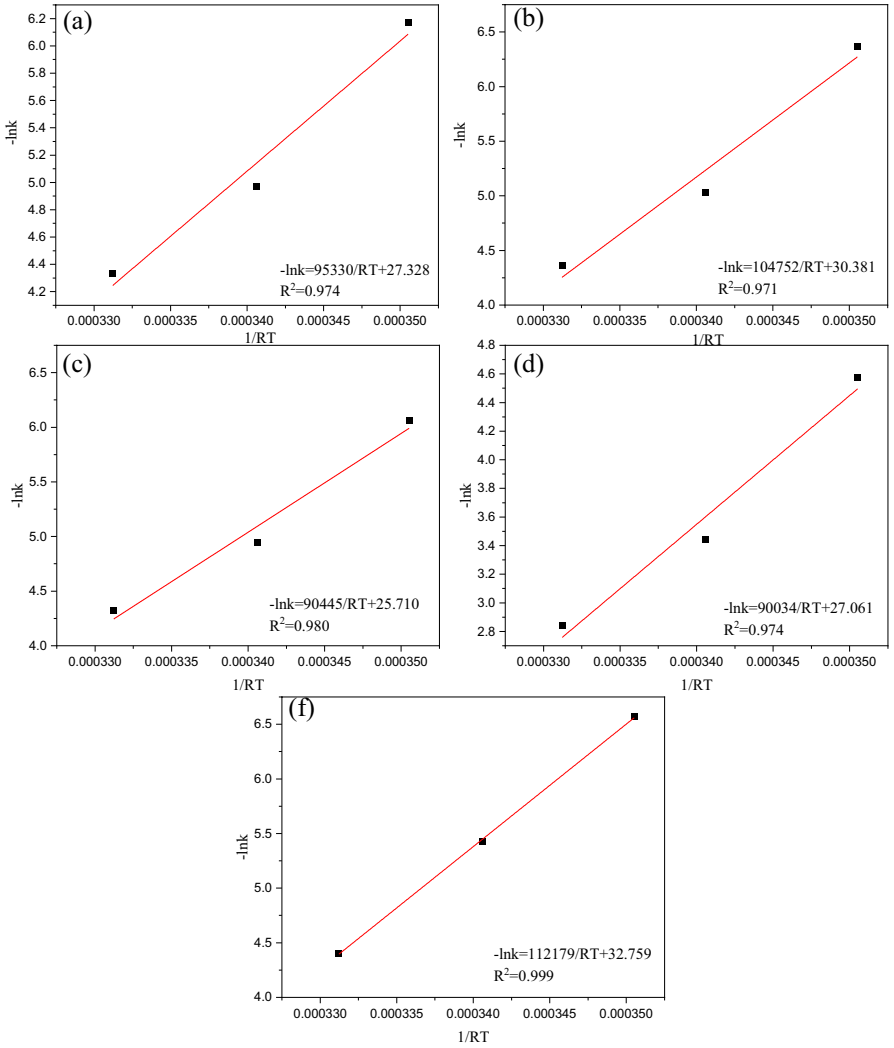

Fig. 2 Arrhenius plots and apparent activation energy for the formation of the product of P1 (**a**), P2 (**b**), P3 (**c**), P4 (**d**) and P5 (**e**) over Hβ in respective reactions. Reaction condition: 5-HMF (0.76 g) reacted with phenol (5.65 g), anisole (6.49 g), guaiacol (7.45 g), cyclohexanone (5.89 g) and acetone (3.48 g) at 343.15 K-363.15 K

Table 2 The apparent activation energies and corresponding R^2 based on the Arrhenius plots for the formations of P1, P2, P3, P4 and P5

Product	Ea (kJ/mol)	R^2
P1 (Ea_1 R_1^2)	95.3(± 15.5)	0.999
P2 (Ea_2 R_2^2)	104.8(± 18.1)	0.971
P3 (Ea_3 R_3^2)	90.4(± 12.9)	0.980
P4(Ea_4 R_4^2)	90.0(± 14.5)	0.974
P5(Ea_5 R_5^2)	112.2(± 1.8)	0.999

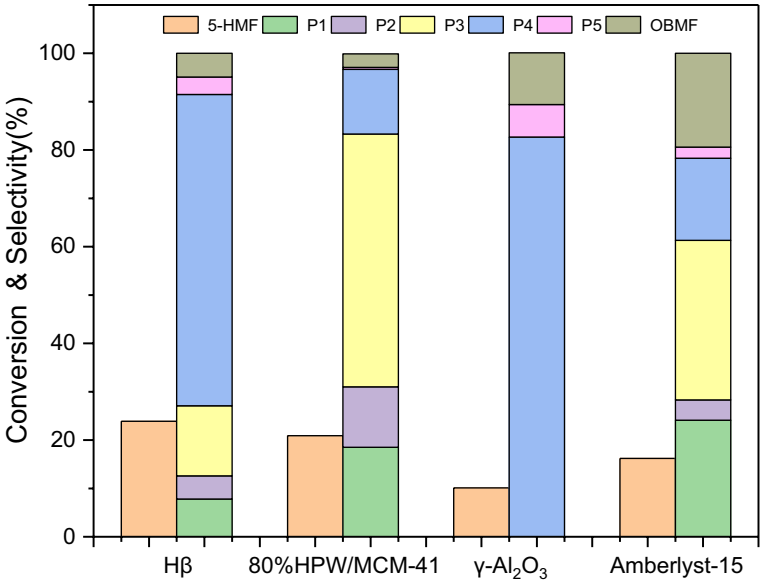

Fig. 3 The conversion of 5-HMF and the selectivity of the products in the mixed reaction of 5-HMF (0.76 g) with phenol (0.98 g), anisole (1.22 g), guaiacol (1.39 g), cyclohexanone (1.10 g) and acetone (0.65 g) by different catalysts at 363.15 K for 6 h

follows the order of Hβ (23.9%) > 80%HPW/MCM-41 (20.9%) > Amberlyst-15 (16.2%) > γ-Al_2O_3 (10.1%), which is in consistence with the acid contents of the catalysis that Hβ (0.97 mmol g^{-1}) > 80%HPW/MCM-41 (0.92 mmol·g^{-1}) > γ-Al_2O_3 (0.51 mmol·g^{-1}) in Table 3, expect Amberlyst-15 (4.13 mmol g^{-1}) because of too small surface area (45 m^2/g). However, the selectivity of products varies greatly. As 80%HPW/MCM-41 was used as catalysis, the selectivity of products is in the order of P3 > P1 > P4 > P2 > P5 with alkylated products content increase tremendously, attributed to the high content of Brønsted acid of 80%HPW/MCM-41. When Amberlyst-15 with weak Brønsted acidity was used as catalyst, the selectivity order of products was also P3 > P1 > P4 > P2 > P5. The lower conversion rate can be attributed to the fact that although Amberlyst-15 resin has a high acid concentration, its acidity is relatively weak and its surface area is small, resulting in lower activity compared to 80%HPW/MCM-41. Under the catalysis of these two catalysts, it tends to produce alkylation products, which indicates that the Brønsted acid site is an effective catalytic active site for the alkylation reaction. When γ-Al_2O_3 was used as catalyst, the product selectivity order was P4 > P5 > P3(0%) = P1(0%) = P2(0%), and no alkylation product was generated. As shown in the Table 4, Brønsted acid is almost undetectable on γ-Al_2O_3, indicating that the Lewis acid site is the active site that is beneficial to the aldol condensation reaction.

It should be noted that the selectivity of P5 is still lower than that of P4 no matter what kind of catalysis is used. In order to interpret this phenomenon, firstly, we calculated the activation sites of 5-HMF. As shown in Fig. 4a and Table 5, found that C11 ($f^+ = 0.1638$) and O15 ($f^+ = 0.1705$) are the most active positions. Therefore, the

Table 3 The surface area, volume and diameter of catalysts by N_2 adsorption and desorption characterization

Samples	S_{BET} (m^2/g)	Vtotal (cm^3/g)	Pore size (nm)
Hβ	494	0.41	3.32
80%TPA/MCM-41	415	0.41	3.95
Amberlyst-15[a]	45[a]	0.31[a]	–
γ-Al_2O_3	139	0.23	6.71

[a]Reference [35]

– Undetected

Table 4 Acid properties of different catalysts

Sample	Acid amount by NH_3-TPD (mmol g^{-1})				Acid amount by pyridine FT-IR (mmol g^{-1}) at 250 ℃			
	Total	Weak	Medium	Strong	B	L	B + L	B/L
Hβ	0.97	0.19	0.33	0.45	0.14	0.23	0.37	0.61
80%TPA/MCM-41	0.92	0.19	0.19	0.54	1.22	0.17	1.39	7.2
Amberlyst-15[a]	4.13[a]	–	–	–	4.13	–	4.13	–
γ-Al_2O_3	0.51	0.29	–	0.29	–	0.20	–	–

[a]Reference [35]

– Undetected

aldehyde group on 5-HMF is the most inclined site for nucleophilic addition (aldol condensation) reactions, indicating that cyclohexanone and acetone as nucleophiles tend to attack the aldehyde group of 5-HMF to generate the condensation products P4 and P5. Subsequently, we obtained that the nucleophilic index of cyclohexanone is 2.74 eV (Fig. 4b, c), which is greater than the nucleophilic index of acetone (2.48 eV). The aldol condensation reaction is a typical nucleophilic addition reaction. The larger the nucleophilic index, the more likely the nucleophilic addition reaction occurs. Therefore, cyclohexanone is easier to attack 5-HMF than acetone, and the aldol condensation reaction occurs to generate the corresponding condensation product [31]. At the same time, we used electronegativity to verify this calculation result. The electronegativity of cyclohexanone is 3.43 eV, which is smaller than 3.55 eV of acetone. The smaller the electronegativity is, the stronger the electron-donating ability is, which is beneficial to the attack of nucleophiles. Therefore, according to theoretical calculations, cyclohexanone is more likely to undergo aldol condensation reaction than acetone with 5-HMF.

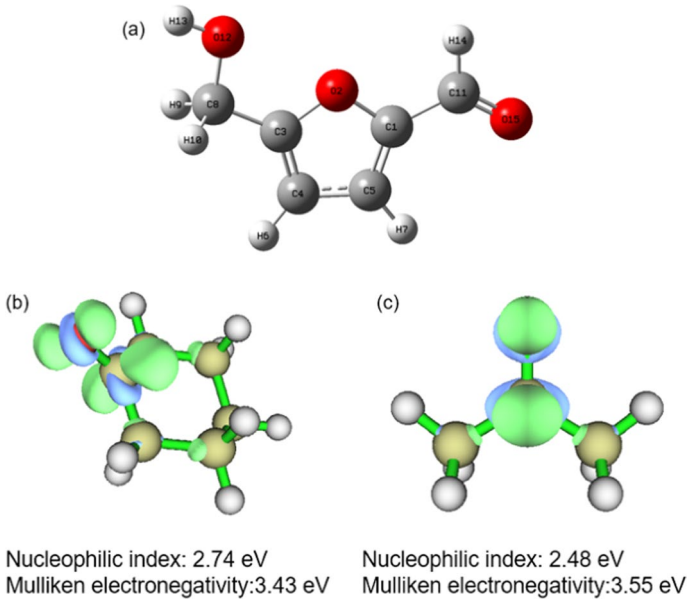

Fig. 4 **A** The chemical structure of 5-HMF, nucleophilic index and Mulliken electronegativity of cyclohexanone (**b**) and acetone (**c**). Computational methods: Calculations are performed using a Gaussian 16 revision C.01. The nucleophilicity index and mulliken electronegativity of cyclohexanone and acetone was predicted by B3LYP/6-31G* basis set combined with Fukui function

Table 5 Natural population analysis (NPA) charge distributions and condensed Fukui index (f^+) of 5-HMF

Atom	q(N)	q(N-1)	q(N + 1)	f^+
C1	0.0369	-0.0159	0.1654	0.0528
O2	-0.0683	-0.1309	-0.0240	0.0626
C3	0.0803	-0.0148	0.1906	0.0951
C4	-0.0794	-0.1356	0.0237	0.0562
C5	-0.0433	-0.1517	0.0354	0.1084
H6	0.0548	0.0124	0.1046	0.0425
H7	0.0667	0.0175	0.1107	0.0492
C8	0.0354	0.0126	0.0710	0.0228
H9	0.0374	0.0039	0.0895	0.0336
H10	0.0375	0.0040	0.0894	0.0334
C11	0.1150	-0.0488	0.1639	0.1638
O12	-0.2303	-0.2419	-0.1789	0.0116
H13	0.1747	0.1501	0.2073	0.0245
H14	0.0383	-0.0383	0.0792	0.0729
C15	-0.2559	-0.4264	-0.1281	0.1705

Conclusion

In this work, one-pot competitive C–C coupling reactions of 5-HMF with other lignocellulose derived chemicals by acid catalysis are interpreted. The apparent activation energies of condensed products of 5-HMF with phenol, anisole, guaiacol, cyclohexanone and acetone are obtained and compared by establishing a kinetic model using Matlab and experiment that 95.3 kJ/mol, 104.8 kJ/mol, 90.4 kJ/mol, 90.0 kJ/mol, 112.2 kJ/mol correspondingly as Hβ as catalysis. Rate of product formation can also be regulated by different catalysis applied that B acid is more beneficial to the alkylation reaction, and L acid preferentially catalyzes the aldol condensation reaction. However, the big discrepancy of nucleophilic index and Mulliken electronegativity of cyclohexanone and acetone makes the aldol condensation difficult to regulate confined by catalysis. This work gives some inspiration for products distribution regulation in the one-pot reaction.

Supplementary Information The online version contains supplementary material available at https://doi.org/10.1007/s11144-024-02622-0.

Acknowledgements This work was supported by the National Natural Science Foundation of China (2210081015), the Natural science Foundation of Shandong Province (ZR2023MB042), the Talent Foundation funded by Province and Ministry Co-construction Collaborative Innovation Center of Eco-chemical Engineering (STHGYX2222), the Open Fund of the Key Laboratory of Multiphase Flow Reaction and Separation Engineering of Shandong Province (2021MFRSE-B01), the Foundation (KF202013) of Key Laboratory of Pulp and Paper Science & Technology of Ministry of Education of China.

Author contributions All authors read and approved the final manuscript. LS: data curation, formal analysis, investigation, methodology, software, writing–original draft. GN: data curation, formal analysis, investigation, methodology, software, writing–original draft. XC: software. HW: resources, software. SL: resources. HY: formal analysis, resources. XL: resources, validation. GY: funding acquisition, investigation, methodology, resources. SY: project administration, resources, supervision, validation, visualization.

Declarations

Competing interests The authors have no competing interests to declare that are relevant to the content of this article.

References

1. Chen S, Wojcieszak R, Dumeignil F, Marceau E, Royer S (2018) How catalysts and experimental conditions determine the selective hydroconversion of furfural and 5-hydroxymethylfurfural. Chem Rev 118:11023–11117. https://doi.org/10.1021/acs.chemrev.8b00134
2. Shen X, Sun R (2021) Recent advances in lignocellulose prior-fractionation for biomaterials, biochemicals, and bioenergy. Carbohydr Polym 261:117884. https://doi.org/10.1016/j.carbpol.2021.117884
3. Pan Z, Li Y, Wang B, Sun F, Xu F, Zhang X (2022) Mild fractionation of poplar into reactive lignin via lignin-first strategy and its enhancement on cellulose saccharification. Bioresour Technol 343:126122. https://doi.org/10.1016/j.biortech.2021.126122
4. Yogalakshmi KN, Sivashanmugam P, Kavitha S, Kannah Y, Varjani S, Adish Kumar S, Kumar G (2022) Lignocellulosic biomass-based pyrolysis: a comprehensive review. Chemosphere 286:131824

5. Amesho KTT, Chen S-C, Wu T-Y, Ponnusamy VK (2023) Green synthesis of 5-hydroxymethylfurfural from biomass-derived carbohydrates using deep eutectic solvents as environmentally benign catalyst. Environ Technol Inno 29:102982. https://doi.org/10.1016/j.eti.2022.102982
6. Niakan M, Masteri-Farahani M, Seidi F (2023) Catalytic fructose dehydration to 5-hydroxymethylfurfural on the surface of sulfonic acid modified ordered mesoporous SBA-16. Fuel 337:127242. https://doi.org/10.1016/j.fuel.2022.127242
7. Niakan M, Masteri-Farahani M, Seidi F (2023) Sulfonated ionic liquid immobilized SBA-16 as an active solid acid catalyst for the synthesis of biofuel precursor 5-hydroxymethylfurfural from fructose. Renew Energy 212:50–56. https://doi.org/10.1016/j.renene.2023.05.064
8. Chen G, Sun Q, Xu J, Zheng L, Rong J, Zong B (2021) Sulfonic derivatives as recyclable acid catalysts in the dehydration of fructose to 5-hydroxymethylfurfural in biphasic solvent systems. ACS Omega 6:6798–6809. https://doi.org/10.1021/acsomega.0c05857
9. Kumar K, Pathak S, Upadhyayula S (2020) 2nd generation biomass derived glucose conversion to 5-hydroxymethylfurfural and levulinic acid catalyzed by ionic liquid and transition metal sulfate: elucidation of kinetics and mechanism. J Clean Prod 256:120292. https://doi.org/10.1016/j.jclepro.2020.120292
10. Kang E-S, Hong Y-W, Chae DW, Kim B, Kim B, Kim YJ et al (2015) From lignocellulosic biomass to furans via 5-acetoxymethylfurfural as an alternative to 5-hydroxymethylfurfural. Chemsuschem 8:1179–1188. https://doi.org/10.1002/cssc.201403252
11. Hafizi H, Walker G, Collins MN (2022) Efficient production of 5-ethoxymethylfurfural from 5-hydroxymethylfurfural and carbohydrates over lewis/brønsted hybrid magnetic dendritic fibrous silica core-shell catalyst. Renew Energy 183:459–471. https://doi.org/10.1016/j.renene.2021.11.036
12. Li Q, Ma C-L, He Y-C (2023) Effective one-pot chemoenzymatic cascade catalysis of biobased feedstock for synthesizing 2,5-diformylfuran in a sustainable reaction system. Bioresour Technol 378:128965. https://doi.org/10.1016/j.biortech.2023.128965
13. Li S, Chen F, Li N, Wang W, Sheng X, Wang A et al (2017) Synthesis of renewable triketones, diketones, and jet-fuel range cycloalkanes with 5-hydroxymethylfurfural and ketones. Chemsuschem 10:711–719. https://doi.org/10.1002/cssc.201601727
14. Arias KS, Climent MJ, Corma A, Iborra S (2015) Synthesis of high quality alkyl naphthenic kerosene by reacting an oil refinery with a biomass refinery stream. Energ Environ Sci 8:317–331. https://doi.org/10.1039/C4EE03194F
15. Nale SD, Jadhav VH (2016) Synthesis of fuel intermediates from HMF/fructose. Catal Lett 146:1984–1990. https://doi.org/10.1007/s10562-016-1836-0
16. Kumar A, Dahotia B, Kumar J, Thallada B (2019) Production of high-density fuel precursor from biomass-derived aromatic oxygenates: effect of N_2 pressure on the alkylation. Ind Eng Chem Res 58:16071–16076. https://doi.org/10.1021/acs.iecr.9b00488
17. Chen S, Zhao C (2021) Production of highly symmetrical and branched biolubricants from lignocellulose-derived furan compounds. ACS Sustain Chem Eng 9:10818–10826. https://doi.org/10.1021/acssuschemeng.1c02875
18. Deng Q, Xu J, Han P, Pan L, Wang L, Zhang X et al (2016) Efficient synthesis of high-density aviation biofuel via solvent-free aldol condensation of cyclic ketones and furanic aldehydes. Fuel Process Technol 148:361–366. https://doi.org/10.1016/j.fuproc.2016.03.016
19. Cueto J, Faba L, Díaz E, Ordóñez S (2017) Performance of basic mixed oxides for aqueous-phase 5-hydroxymethylfurfural-acetone aldol condensation. Appl Catal B 201:221–231. https://doi.org/10.1016/j.apcatb.2016.08.013
20. Jing Y, Xin Y, Guo Y, Liu X, Wang Y (2019) Highly efficient Nb_2O_5 catalyst for aldol condensation of biomass-derived carbonyl molecules to fuel precursors. Chin J Catal 40:1168–1177. https://doi.org/10.1016/S1872-2067(19)63371-1
21. Tampieri A, Russo C, Marotta R, Constantí M, Contreras S, Medina F (2021) Microwave-assisted condensation of bio-based hydroxymethylfurfural and acetone over recyclable hydrotalcite-related materials. Appl Catal B 282:119599. https://doi.org/10.1016/j.apcatb.2020.119599
22. Malkar RS, Daly H, Hardacre C, Yadav GD (2019) Aldol condensation of 5-hydroxymethylfurfural to fuel precursor over novel aluminum exchanged-DTP@ZIF-8. ACS Sustain Chem Eng 7:16215–16224. https://doi.org/10.1021/acssuschemeng.9b02939
23. Xia Q-N, Cuan Q, Liu X-H, Gong X-Q, Lu G-Z, Wang Y-Q (2014) $Pd/NbOPO_4$ multifunctional catalyst for the direct production of liquid alkanes from aldol adducts of furans. Angew Chem Int Ed 53:9755–9760. https://doi.org/10.1002/anie.201403440

24. Bui TV, Sooknoi T, Resasco DE (2017) Simultaneous upgrading of furanics and phenolics through hydroxyalkylation/aldol condensation reactions. Chemsuschem 10:1631–1639. https://doi.org/10.1002/cssc.201601251
25. Li S, Cao J, Feng X, Du Y, Yang C, Xu W (2021) Computation-guided descriptor for efficient zeolite catalysts screening in C4 alkylation process. Chem Eng Sci 241:116726. https://doi.org/10.1016/j.ces.2021.116726
26. Taghavi S, Pizzolitto C, Ghedini E, Menegazzo F, Cruciani G, Peurla M et al (2023) Levulinic acid production: comparative assessment of Al-rich ordered mesoporous silica and microporous zeolite. Catal Lett 153:41–53. https://doi.org/10.1007/s10562-022-03955-y
27. Tian X, Zeng Z, Liu Z, Dai L, Xu J, Yang X et al (2022) Conversion of low-density polyethylene into monocyclic aromatic hydrocarbons by catalytic pyrolysis: comparison of HZSM-5, Hβ, HY and MCM-41. J Clean Prod 358:131989. https://doi.org/10.1016/j.jclepro.2022.131989
28. Kikhtyanin O, Bulánek R, Frolich K, Čejka J, Kubička D (2016) Aldol condensation of furfural with acetone over ion-exchanged and impregnated potassium BEA zeolites. J Mol Catal A 424:358–368. https://doi.org/10.1016/j.molcata.2016.09.014
29. Shen Z, Zhang G, Shi C, Qu J, Pan L, Huang Z et al (2023) Bifunctional Pt/Hβ catalyzed alkylation and hydrodeoxygenation of phenol and cyclohexanol in one-pot to synthesize high-density fuels. Fuel 334:126634. https://doi.org/10.1016/j.fuel.2022.126634
30. Li Q, Nie G, Wang H, Zou J-J, Yu S, Yu H et al (2023) Synthesis of high-grade jet fuel blending precursors by aldol condensation of lignocellulosic ketones using HfTPA/MCM-41 with strong acids and enhanced stability. Appl Catal B 325:122330. https://doi.org/10.1016/j.apcatb.2022.122330
31. Zhang H, Xie C, Chen L, Duan J, Li F, Liu W (2023) Different reaction mechanisms of $SO4^{\bullet-}$ and •OH with organic compound interpreted at molecular orbital level in Co(II)/peroxymonosulfate catalytic activation system. Water Res 229:119392. https://doi.org/10.1016/j.watres.2022.119392
32. Lu T, Chen F (2012) Multiwfn: a multifunctional wavefunction analyzer. J Comput Chem 33:580–592. https://doi.org/10.1002/jcc.22885
33. Nie G, Li G, Liang D, Zhang X (2017) Alkylation of toluene with cyclohexene over phosphotungstic acid: a combined experimental and computational study. J Catal 355:145–155. https://doi.org/10.1016/j.jcat.2017.09.008
34. Jackson LB (1996) Digital filters and signal processing, with MATLAB® exercises
35. Zhang X, Deng Q, Han P, Xu J, Pan L, Wang L et al (2017) Hydrophobic mesoporous acidic resin for hydroxyalkylation/alkylation of 2-methylfuran and ketone to high-density biofuel. AIChE J 63:680–688. https://doi.org/10.1002/aic.15410

Authors and Affiliations

Linyan Song[1] · Genkuo Nie[1,2] · Xiulei Chen[1] · Hongyu Wang[3] · Shiwei Liu[1] · Hailong Yu[1] · Xuguang Liu[4] · Guihua Yang[2] · Shitao Yu[1]

✉ Genkuo Nie
niegenkuo@qust.edu.cn

[1] Key Laboratory of Multiphase Flow Reaction and Separation Engineering of Shandong Province, College of Chemical Engineering, Qingdao University of Science and Technology, 53 Zhengzhou Road, Qingdao 266042, China

[2] Key Laboratory of Pulp and Paper Science & Technology of Ministry of Education, Qilu University of Technology (Shandong Academy of Sciences), Jinan 250353, China

[3] State Key Laboratory of Safety and Control for Chemicals, SINOPEC Research Institute of Safety Engineering, Qingdao 266071, China

[4] College of Materials Science and Engineering, Qingdao University of Science and Technology, 53 Zhengzhou Road, Qingdao 266042, China